# Numerical Simulation on Temperature Distribution of Steam Generator under Tube Plugging Conditions

Jonggan Hong*, Seungho Ryu, Ji-Woong Han
*Korea Atomic Energy Research Institute, 111, Daedeok-daero 989beon-gil, Yuseong-gu, Daejeon, 34057, Korea*
**Corresponding author: hong@kaeri.re.kr*

## 1. Introduction

In the 150-MWe Korean prototype SFR, a once-through type, shell-and-tube heat exchanger with straight vertical tubes was adopted for steam generators. Reliable operation of the steam generators has been a key issue through operating experience of foreign sodium-cooled fast reactors because it is one of the most important components deciding the plant availability and reliability.

The temperature differences between parts of the 196-MWt large scale steam generator during operation have to be carefully estimated because it has a number of long and straight tubes. Non-uniformity in sodium flow and temperature distributions might cause mechanical integrity problems such as tube buckling and tube-to-tube sheet junction failure in the straight tubes. According to previous studies [1-4], the flow distribution in the inlet plenum of the sodium-heated steam generator was assessed, and proper flow distributors were designed to make uniform sodium flow distribution. The temperature distributions at the tube bundle region under normal operation and plugged tube conditions were also evaluated to figure out thermal expansion mismatch between tubes. In India, a model steam generator was tested in the Steam Generator Test Facility (SGTF) to validate the thermal hydraulic and mechanical designs [5]. In KAERI, numerical thermal hydraulic analyses for PGSFR SG were carried out to select the porosity of the flow distributors at the inlet plenum and assess the sodium and tube temperatures during normal operation [6,7].

This work focuses on a numerical study on the temperature distribution at tube bundle of the steam generator for PGSFR with the STAR-CCM+ CFD package coupled with the HSGSA code. In particular, the simulations under various plugged tube conditions were carried out to evaluate the effect of the tube plugging on the temperature distribution.

## 2. Methods and Results

### *2.1 Domain of Analysis*

A 30˚ sector domain of the tube bundle region in the steam generator was analyzed to acquire the axial and radial sodium temperature distributions (Fig. 1a). The only sodium region of the tube bundle part was modeled in the analysis domain. The hot sodium circumferentially enters the top of the tube bundle and flows downwards. 27 tube support plates which are located at equidistant intervals along the tube hold the tubes and help to make the flow uniform. The sodium transfers heat to the tubes, cools down, and exits radially at the bottom of the tube bundle.

A polyhedral mesh with prism layer cells was employed and the number of cells was about 20 million (Fig 1b). The cell number and quality of the mesh were selected through a mesh dependency study. The average Y+ on the surface of the tubes and the whole walls were evaluated to be about 30.9 and 39.2, respectively.

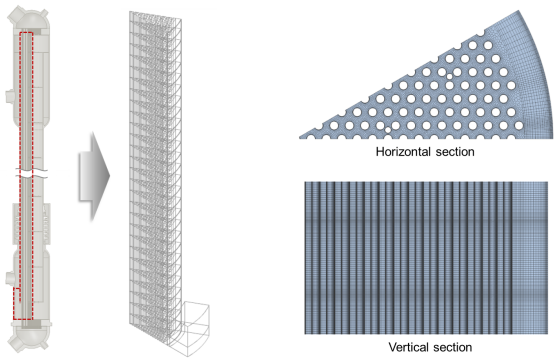


(a) (b)

Fig. 1. Analysis domain of tube bundle region and sectional views of mesh.

### *2.2 HSGSA Code*

HSGSA is one-dimensional fortran code used for thermal sizing of the steam generator. It was developed for the design and performance analysis of the shell-and-tube type steam generator with straight tube arrangement. A single flow channel associated with an individual heat transfer tube was basically considered for thermal sizing and then calculation results and design variables regarding heat transfer and pressure drop were extended to a number of tubes. The analysis domain was discretized into tens of control volumes, and heat transfer and pressure losses were calculated in each control volume. Conservation equations for the mass, momentum, and energy balance for both the shell- and tube-sides fluid flow were solved. The empirical correlations of the heat transfer and pressure drop were used for each boiling regime of the water side and single phase flow of the sodium side. The shell- and tube-sides were coupled by analyzing the heat transfer between them. The overall heat transfer coefficient based on the log-mean temperature difference method was

determined in each control volume. The thermal resistances in the heat transfer path such as convection resistances both on the shell- and tube-sides, conduction resistance in the tube wall, and fouling resistances on the wall surfaces of the tube were taken into account.

### *2.3 Computational Analysis*

To calculate the sodium temperature distributions and tube temperature profiles, the sodium side was analyzed with STAR-CCM+ V11.02.009 and the water/steam side was estimated with the one-dimensional HSGSA code. An iterative calculation scheme which is similar to the one introduced in the previous Indian study [4] was employed. Initially, the heat flux profiles along each tube wall were obtained by calculating two-phase heat transfer of the water side with the HSGSA code. Those results were applied as heat flux boundary conditions on the tube walls in the STAR-CCM+ simulation. Then, radial temperature distribution obtained from STAR-CCM+ was taken into the input of HSGSA. The inlet and exit sodium temperatures for each tube were calculated and used in the HSGSA to determine the heat flux boundary conditions of each tube for the next sequence. The iterative calculation was conducted until convergence criteria that the sodium exit temperatures of each tube should change within 1% deviation compared to the previous iteration was met.

The $k$-$\omega$ SST model was adopted by the turbulence model dependency study. A uniform velocity profile was assumed as sodium inlet boundary condition based on the radial velocity profiles at the tube bundle entrance region acquired in the previous study [7]. A pressure outlet was applied as outlet boundary condition. For normal operation, inlet temperature conditions for the sodium and feedwater were set to be 533℃ and 240℃, respectively. The tube support plates were treated as porous baffle interfaces, and the pressure drop model for their porous inertial resistances was calculated by a separate pressure drop simulation for the tube support plates.

Under normal operation condition, five tube plugging cases were simulated and the calculation results were compared (Table I). Fig 2 displays the position of the plugged tubes. Adiabatic boundary condition was applied to the walls of the plugged tubes.

Table I: Simulation cases for plugging conditions

| Case # | Description | Plugged tube position |
|---|---|---|
| 1 | No plugging | - |
| 2 | 1 central tube plugging | 1 |
| 3 | 7 central tubes plugging | 1, 2 |
| 4 | 2 peripheral tubes plugging | 60, 67 |
| 5 | 7 intermediate tubes plugging | 53, 54, 61, 62 |
| 6 | 5 peripheral tubes plugging | 59, 60, 66, 67, 72 |

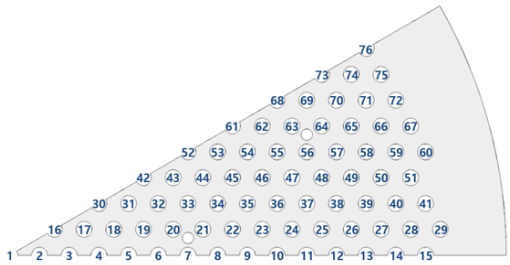


Fig. 2. Diagram for tube position.

### *2.4 Results and Discussion*

As shown in Fig. 3a, the 27 tube support plates made uniform sodium flow distribution at the tube bundle region. In addition, a baffle structure in the periphery of the tube support plate generated recirculation in sodium by-pass flow. The mixing effect by the baffles in the periphery was obviously displayed in a vertical temperature distribution (Fig. 3b). The sodium temperature distribution at the tube bundle was relatively uniform in radial because the sodium flow was uniform by the tube support plate. However, the sodium temperature in the periphery was hotter than that in the tube bundle due to the influence of the sodium by-pass. Fig. 4 shows the radial temperature distributions at each height under the normal operating condition (case #1). The temperature deviation between the central and peripheral parts increased gradually as the sodium went down from the top part to the middle part. In the bottom part, relatively uniform temperature distribution in radial was achieved due to the cross flow effect at the exit.

In the case of the tube plugging cases #2-6, the flow distribution like Fig. 3a was rarely affected by the plugged tubes. However, the sodium temperature around the plugged tubes increased significantly. In Fig. 3c, the sodium temperatures of the central part were much hotter than those of Fig. 3b because of the seven central tubes plugging. This local temperature increase was obviously observed on horizontal sections as well (Fig. 5). The horizontal temperature distributions were obtained at a height of 12.23 m from the bottom (total length: ~ 25 m). The temperature rise around the adjacent normal tubes was found to be negligible.

Fig. 6 shows that the average temperature of the plugged tubes was much higher than that of the normal tubes. In Table II, the average temperatures of the normal tubes, plugged tubes, central tubes (position: 1 and 2), and peripheral tubes (position: 15, 29, 41, 51, 60, 67, 72, 75, and 76) for each simulation case were compared. A major factor to increase the temperature of the plugged tubes was not the location of the plugged tubes, but how many plugged tubes were gathered in one place. As the number of the plugged tubes locally gathered increased from one to seven, the difference between the average temperature of the normal and

plugged tubes increased approximately from 8℃ to 59℃. During normal operation, the radial temperature difference by peripheral by-pass sodium flow caused the average temperature difference of 18℃ between the central tubes and peripheral tubes. The average temperature difference between the central tubes and peripheral tubes became larger as the plurality of the plugged tubes are gathered in one place and the tubes are located at the center rather than the periphery. Under the seven central plugged tubes condition, the average temperature difference between the central tubes and peripheral tubes turned out to be the maximum value of about 56℃.

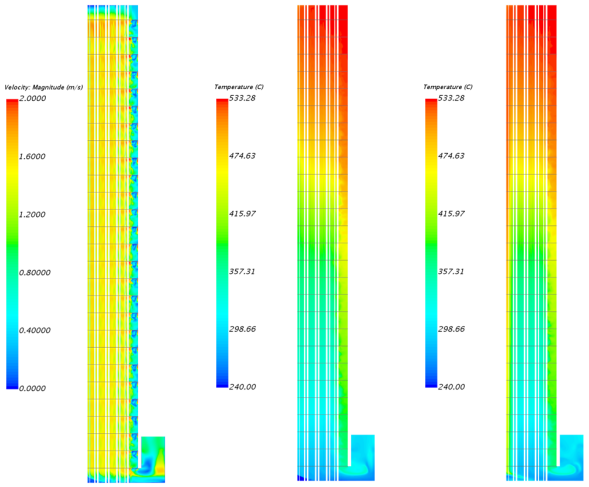


(a) (b) (c)

Fig. 3. Flow and temperature distributions on vertical sections: (a) case #1 – flow distribution; (b) case #1 – temperature distribution; (c) case #3 – temperature distribution.

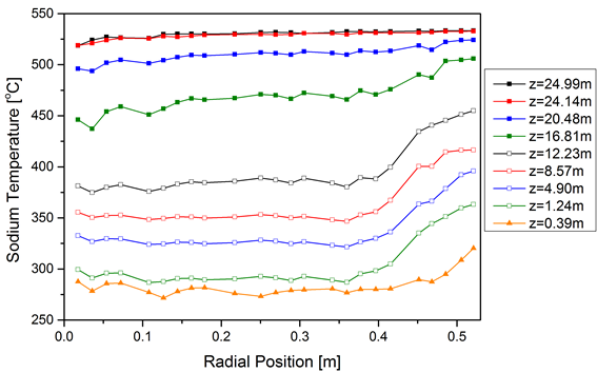


Fig. 4. Radial sodium temperature distribution (case #1).

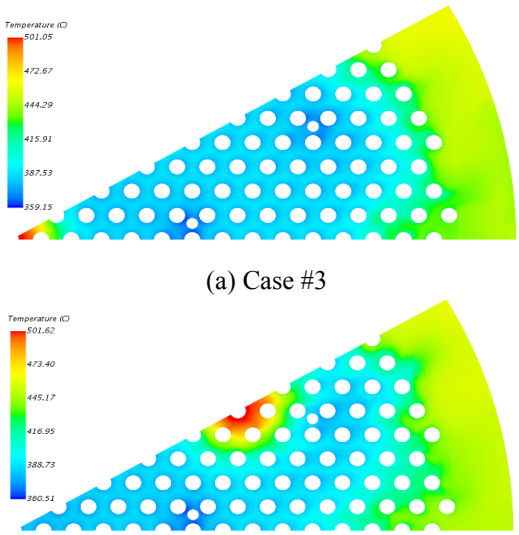


(a) Case #3

(b) Case #5

Fig. 5. Temperature distributions on horizontal sections.

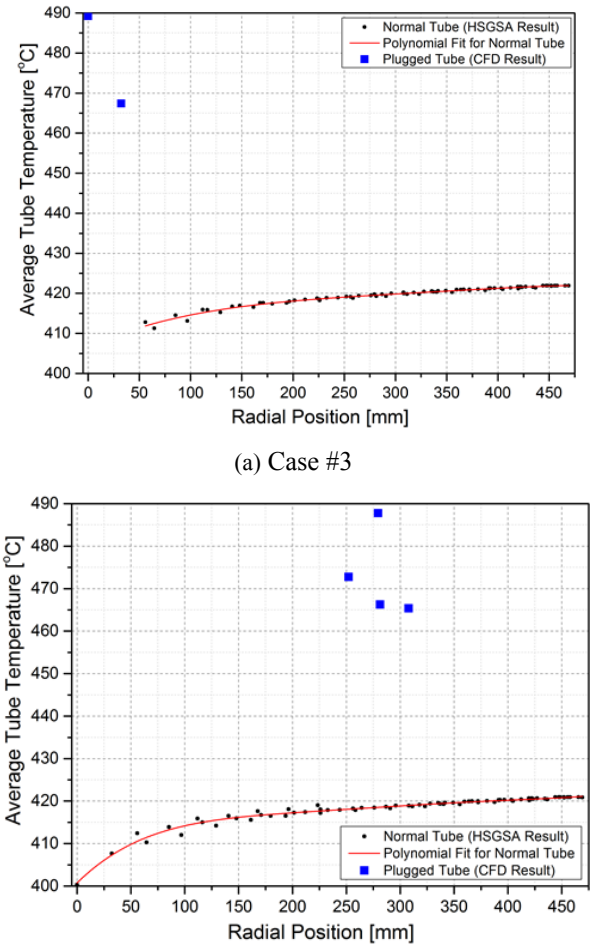


(a) Case #3

(b) Case #5

Fig. 6. Average tube temperature distribution.

Table II: Comparison of tube temperatures

| Case # / Temp. (℃) | 1 | 2 | 3 | 4 | 5 | 6 |
|---|---|---|---|---|---|---|
| Average temp. of normal tubes [A] | 419.5 | 419.6 | 419.6 | 418.9 | 418.2 | 416.8 |
| Average temp. of plugged tubes [B] | - | 427.9 | 478.3 | 457.7 | 473.0 | 466.0 |
| B - A | - | 8.3 | 58.7 | 38.8 | 54.8 | 49.2 |
| Average temp. of central tubes [C] | 404.2 | 418.0 | 478.3 | 404.2 | 404.0 | 401.7 |
| Average temp. of peripheral tubes [D] | 422.3 | 422.1 | 421.9 | 429.6 | 420.9 | 437.3 |
| D - C | 18.1 | 4.1 | -56.4 | 25.4 | 16.9 | 35.6 |

## 3. Conclusions

A numerical study on the temperature distribution at tube bundle of the steam generator for PGSFR with the STAR-CCM+ CFD package coupled with the HSGSA code. In particular, the simulations under various plugged tube conditions were carried out to evaluate the effect of the tube plugging on the temperature distribution. Based on the results of this work, the mechanical structure analysis of the PGSFR steam generator will be carried out to evaluate the integrity of the component.

## ACKNOWLEDGMENT

This work was supported by the National Research Foundation of Korea (NRF) grant funded by the Korean Government (MSIP). (No. 2012M2A8A2025624)

## REFERENCES

[1] N. Kisohara, T. Moribe, and T. Sakai, Temperature and Flow Distributions in Sodium-heated Large Straight Tube Steam Generator by Numerical Methods, Nuclear Technology, Vol. 164, p. 103, 2008.
[2] L. T. Patil, A. W. Patwardhan, G. Padmakumar, and G. Vaidyanathan, Distribution of Liquid Sodium in the Inlet Plenum of Steam Generator in a Fast Breeder Reactor, Nuclear Engineering and Design, Vol. 240, p. 850, 2010.
[3] H. P. Khadamakar, A. W. Patwardhan, G. Padmakumar, and G. Vaidyanathan, Flow Distribution in the Inlet Plenum of Steam Generator, Nuclear Engineering and Design, Vol. 241, p. 4165, 2011.
[4] R. Nandakumar, P. Selvaraj, S. Athmalingam, V. Balasubramaniyan, and S. C. Chetal, Thermal Simulation of Sodium Heated Once through Steam Generator for a Fast Reactor, Int J Adv Eng Sci Appl Math, Vol. 4, p. 127, 2012.
[5] V. Vinod, L. S. Sivakumar, V. A. Suresh Kumar, I. B. Noushad, G. Padmakumar, K. K. Rajan, Experiemental Evaluation of the Heat Transfer Performance of Sodium Heated Once through Steam Generator, Nuclear Engineering and Design, Vol. 273, p. 412, 2014.
[6] J. Hong, S. Ryu, T. H. Lee, Thermal Hydraulic Study of Steam Generator of PGSFR, International Conference on Fast Reactors and Related Fuel Cycles: Next Generation Nuclear Systems for Sustainable Development (FR17), 26-29 June, 2017, Yekaterinburg, Russian Federation.
[7] J. Hong, S. Ryu, M. Kim, J. W. Han, Numerical Simulation on Flow Distribution in Inlet Plenum of Steam Generator, Transactions of the Korean Nuclear Society Autumn Meeting, 26-27 Oct., 2017, Gyeongju, Korea.